

SYSTEMATIC ANALYSIS OF THE D-WAVE CHARMONIUM STATES WITH THE QCD SUM RULES

Qi Xin ¹, Zhi-Gang Wang ²

Department of Physics, North China Electric Power University, Baoding 071003, P. R. China

Abstract

We systematically study the 1D charmonium spin-triplet (with the $J^{PC} = 1^{--}, 2^{--}, 3^{--}$) and spin-singlet (with the $J^{PC} = 2^{-+}$) via the QCD sum rules in comparison with the recent experimental results. The predicted mass $M_{\psi_1} = 3.77 \pm 0.09$ GeV supports identifying the ψ_1 as the $\psi(3770)$, the value $M_{\psi_2} = 3.82 \pm 0.09$ GeV is consistent with the reported observation of the $\psi_2(3823)$, the prediction $M_{\psi_3} = 3.84 \pm 0.08$ GeV supports identifying the ψ_3 as the $\psi_3(3842)$. Additionally, we estimate the unobserved η_{c2} state lies at 3.83 ± 0.09 GeV, and suggest detection prospects in the future. More experimental data will help us to unravel the mass spectrum of the charmonium states near the open-charm thresholds.

PACS number: 12.39.Mk, 12.38.Lg

Key words: Charmonium, QCD sum rules, D-wave

1 Introduction

Charmonium, a flavorless meson made of a charmed quark and its antiquark, provides an ideal system for studying QCD up to the non-perturbative regime. Its study offers us an excellent topic to investigate strong interactions. Therefore, systematically exploring the charmonium states can deepen our understanding of the dynamics involving the heavy quarkonium systems. Since the observation of the J/ψ in 1974 [1, 2], experimental and theoretical physicists have actively wrestling with the charmonium states. Prior to the discovery of the $X(3872)$ in 2003 [3], many charmonium states, such as the $\eta_c, \eta'_c, J/\psi, \psi', h_c, \chi_{c0}, \chi_{c1}, \chi_{c2}, \psi(3770), \psi(4040), \psi(4415)$, etc, were reported by the experimental collaborations [4, 5, 6, 7, 8, 9, 10], which can be classified in the traditional quark model. In fact, as early as the 1980s, the theoretical physicists began to focus on those particles and examined the mass spectrum, decay modes and collision processes in detail [11, 12, 13, 14].

The 1^3D_1 charmonium candidate was observed with the mass 3772 ± 6 MeV in 1977 [15]. In 2004, the Belle collaboration firstly reported the $\psi(3770)$ in the process $B^+ \rightarrow \psi(3770)K^+$ with the decay modes $\psi(3770) \rightarrow D^0\bar{D}^0/D^+D^-$ [16]. On the other hand, the BESIII collaboration recently observed the $\mathcal{R}(3780)$ with the mass $M_{\mathcal{R}(3780)} = 3778.7 \pm 0.5 \pm 0.3$ MeV and the decay width $\Gamma_{\mathcal{R}(3780)} = 20.8 \pm 0.8 \pm 1.7$ MeV, which can also be interpreted as the 1^3D_1 charmonium state [17].

The D-wave charmonium with the quantum numbers $J^{PC} = 2^{--}$ has been explored experimentally several times, the Belle collaboration observed an evidence of a resonance with statistical significance of 3.8σ in the $\chi_{c1}\gamma$ final state, whose mass is $3823.1 \pm 1.8 \pm 0.7$ MeV [20], and the BESIII collaboration reported the $X(3823)$ in the process $e^+e^- \rightarrow \pi^+\pi^-X(3823) \rightarrow \pi^+\pi^-\gamma\chi_{c1}$ with a statistical significance of 6.2σ , the measured mass is $3821.7 \pm 1.3 \pm 0.7$ MeV [21]. In 2020, the LHCb collaboration measured the energy gaps among the $\psi_2(3823), \chi_{c1}(3872)$ and $\psi(2S)$ states [22]. While the BESIII collaboration precisely measured the mass of the $\psi_2(3823)$ to be $3823.12 \pm 0.43 \pm 0.13$ MeV/ $3824.5 \pm 2.4 \pm 1.0$ MeV [23, 24].

In the decay modes $X(3842) \rightarrow D^0\bar{D}^0$ and D^+D^- , a new narrow charmonium state named as $X(3842)$ was detected by the LHCb collaboration with very high statistical significance. Its determined mass and width are $3842.71 \pm 0.16 \pm 0.12$ MeV and $2.79 \pm 0.51 \pm 0.35$ MeV, respectively [25], which imply that the $X(3842)$ state might be the $\psi_3(1^3D_3)$ charmonium state with the spin-parity-charge-conjugation $J^{PC} = 3^{--}$. While the 1^1D_2 charmonium state has not been observed yet.

¹E-mail: xinqihd@163.com.

²E-mail: zgwang@aliyun.com.

L	states	J^{PC}	currents
S-wave	η_c	0^{-+}	$\bar{c}(x)i\gamma_5 c(x)$
	J/ψ	1^{--}	$\bar{c}(x)\gamma_\mu c(x)$
P-wave	χ_{c0}	0^{++}	$\bar{c}(x)c(x)$
	χ_{c1}	1^{++}	$\bar{c}(x)\gamma_\mu\gamma_5 c(x)$
	h_c	1^{+-}	$\bar{c}(x)\sigma_{\mu\nu}c(x)$
	χ_{c2}	2^{++}	$\bar{c}(x)(\gamma_\mu\partial_\nu + \gamma_\nu\partial_\mu - \frac{1}{2}g_{\mu\nu}\not{\partial})c(x)$
D-wave	ψ_1	1^{--}	$J_\mu(x)$ in Eq.(2)
	ψ_2	2^{--}	$J_{\mu\nu}^1(x)$ in Eq.(2)
	η_{c2}	2^{-+}	$J_{\mu\nu}^2(x)$ in Eq.(2)
	ψ_3	3^{--}	$J_{\mu\nu\rho}(x)$ in Eq.(2)

Table 1: The quantum numbers and interpolating currents of the charmonia.

In 2023, the BESIII collaboration observed three resonance structures $\mathcal{R}(3760)$, $\mathcal{R}(3780)$ and $\mathcal{R}(3810)$ in the cross sections for the process $e^+e^- \rightarrow$ non open charm hadrons with significances of 9.4σ , 15.7σ , and 9.8σ , respectively [26], they observed the $\mathcal{R}(3810)$ for the first time [26], and confirmed the old particles $\mathcal{R}(3760)$ and $\mathcal{R}(3780)$ [27]. The experimental masses and widths were measured to be $M_{\mathcal{R}(3760)} = 3761.7 \pm 2.2 \pm 1.2$ MeV, $\Gamma_{\mathcal{R}(3760)} = 6.7 \pm 11.1 \pm 1.1$ MeV, $M_{\mathcal{R}(3780)} = 3784.7 \pm 5.7 \pm 1.6$ MeV, $\Gamma_{\mathcal{R}(3780)} = 31.6 \pm 11.9 \pm 3.2$ MeV, $M_{\mathcal{R}(3810)} = 3805.8 \pm 1.1 \pm 2.7$ (3805.8 \pm 1.1 \pm 2.7) MeV, $\Gamma_{\mathcal{R}(3810)} = 11.6 \pm 2.9 \pm 1.9$ (11.5 \pm 2.8 \pm 1.9) MeV [26]. And those parameters were improved recently, $M_{\mathcal{R}(3760)} = 3751.9 \pm 3.8 \pm 2.8$ MeV, $\Gamma_{\mathcal{R}(3760)} = 32.8 \pm 5.8 \pm 8.7$ MeV, $M_{\mathcal{R}(3780)} = 3778.7 \pm 0.5 \pm 0.3$ MeV, $\Gamma_{\mathcal{R}(3780)} = 20.3 \pm 0.8 \pm 1.7$ MeV, $M_{\mathcal{R}(3810)} = 3804.5 \pm 0.9 \pm 0.9$ MeV, $\Gamma_{\mathcal{R}(3810)} = 5.4 \pm 3.5 \pm 3.2$ MeV [17].

In our previous works, we have adopted the QCD sum rules approach as a valuable theoretical tool to describe the masses, pole residues, form-factors, hadronic coupling constants and decay widths for the charmed mesons D , D^* , D_s , D_s^* , $D_0^*(2400)$, $D_{s0}^*(2317)$, $D_1(2430)$, $D_{s1}(2460)$, $D_{s1}^*(2860)$, $D_{s3}^*(2860)$ [28, 29, 30], charmonium or charmonium-like states $X(3842)$, $X(3872)$, $h_c(4000)$, $\chi_{c1}(4010)$, and so on [31, 33, 34, 35, 36, 37]. The masses of those charmonium-like states lie near the open-charm meson-pair thresholds, therefore they have been identified as the charmonia, tetraquark states, molecular states etc, more theoretical and experimental investigations are still needed to understand the mass spectrum of the charmonium states.

The S-wave and P-wave charmonium states have been comprehensively explored in the framework of the QCD sum rules, we summarize the interpolating currents in Table 1, however, the systematic study of the D-wave charmonium states via the QCD sum rules method is still scarce [31], we would focus on this subject.

For other theoretical works on the D-wave charmonium mass spectrum, one can consult the Bethe-Salpeter equations [32], nonrelativistic potential model [39] (include the screened potential model [40, 41], the linear potential model [41, 42], the Coulomb plus linear potential model [43]), the relativized Godfrey-Isgur model [38, 39], the relativistic screened potential model [44], the unquenched potential model [45], the Cornell potential (coupled-channel) model (with relativistic correction) [14, 46]([47]), the coupled-channel model [48], the QCD-motivated relativistic quark model based on the quasipotential approach [49] and the other potential model [50, 51, 52, 53].

The paper is arranged as follows: in Sect.2, we obtain the QCD sum rules for the D-wave charmonium states; in Sect.3, we provide a comprehensive analysis; and in Sect.4, we give a short summary.

2 QCD sum rules for the D-wave charmonium states

The two-point correlation functions can be written as,

$$\begin{aligned}
\Pi_{\mu\nu}(p) &= i \int d^4x e^{ip \cdot x} \langle 0 | T \{ J_\mu(x) J_\nu^\dagger(0) \} | 0 \rangle, \\
\Pi_{\mu\nu\alpha\beta}(p) &= i \int d^4x e^{ip \cdot x} \langle 0 | T \{ J_{\mu\nu}(x) J_{\alpha\beta}^\dagger(0) \} | 0 \rangle, \\
\Pi_{\mu\nu\rho\alpha\beta\sigma}(p) &= i \int d^4x e^{ip \cdot x} \langle 0 | T \{ J_{\mu\nu\rho}(x) J_{\alpha\beta\sigma}^\dagger(0) \} | 0 \rangle,
\end{aligned} \tag{1}$$

where the interpolating currents, $J_{\mu\nu}(x) = J_{\mu\nu}^1(x), J_{\mu\nu}^2(x)$,

$$\begin{aligned}
J_\mu(x) &= \bar{c}(x) \overleftrightarrow{D}_\alpha \overleftrightarrow{D}_\beta \gamma_\rho (g^{\alpha\beta} g^{\rho\mu} + g^{\alpha\rho} g^{\beta\mu} + g^{\rho\beta} g^{\alpha\mu}) c(x), \\
J_{\mu\nu}^1(x) &= \bar{c}(x) \left(\gamma_\mu \gamma \cdot \overleftrightarrow{D} \overleftrightarrow{D}_\nu + \gamma_\mu \overleftrightarrow{D}_\nu \gamma \cdot \overleftrightarrow{D} + \gamma_\nu \gamma \cdot \overleftrightarrow{D} \overleftrightarrow{D}_\mu + \gamma_\nu \overleftrightarrow{D}_\mu \gamma \cdot \overleftrightarrow{D} - g_{\mu\nu} \gamma \cdot \overleftrightarrow{D} \gamma \cdot \overleftrightarrow{D} \right) \gamma_5 c(x), \\
J_{\mu\nu}^2(x) &= \bar{c}(x) \left(\overleftrightarrow{D}_\mu \overleftrightarrow{D}_\nu + \overleftrightarrow{D}_\nu \overleftrightarrow{D}_\mu - \frac{1}{2} g_{\mu\nu} \overleftrightarrow{D} \cdot \overleftrightarrow{D} \right) \gamma_5 c(x), \\
J_{\mu\nu\rho}(x) &= \bar{c}(x) \left(\overleftrightarrow{D}_\mu \overleftrightarrow{D}_\nu \gamma_\rho + \overleftrightarrow{D}_\rho \overleftrightarrow{D}_\mu \gamma_\nu + \overleftrightarrow{D}_\nu \overleftrightarrow{D}_\rho \gamma_\mu \right) c(x),
\end{aligned} \tag{2}$$

the covariant derivative $\overleftrightarrow{D}_\mu = \overrightarrow{\partial}_\mu - ig_s G_\mu - \overleftarrow{\partial}_\mu - ig_s G_\mu$, and the G_μ is the gluon field. We take two- $\overleftrightarrow{D}_\mu$ to represent the D-wave to construct the currents $J_\mu(x)$, $J_{\mu\nu}^1(x)$, $J_{\mu\nu}^2(x)$ and $J_{\mu\nu\rho}(x)$ to interpolate the charmonium states ψ_1 , ψ_2 , η_{c2} and ψ_3 respectively. The quark currents with the covariant derivative $\overleftrightarrow{D}_\mu$ are gauge invariant, although which blurs the physical interpretation of the $\overleftrightarrow{D}_\mu$ being the angular momentum.

To obtain the hadronic representation, we insert a complete set of intermediate hadronic states with the same quantum numbers as the current operators $J_\mu(x)$, $J_{\mu\nu}(x)$ and $J_{\mu\nu\rho}(x)$ into the correlation functions $\Pi_{\mu\nu}(p)$, $\Pi_{\mu\nu\alpha\beta}(p)$ and $\Pi_{\mu\nu\rho\alpha\beta\sigma}(p)$ [30, 54, 55, 56], and consider the current-hadron couplings,

$$\begin{aligned}
\langle 0 | J_\mu(0) | \psi_1(p) \rangle &= f_{\psi_1} \varepsilon_\mu, \\
\langle 0 | J_\mu(0) | \chi_{c0}(p) \rangle &= f_{\chi_{c0}} p_\mu,
\end{aligned} \tag{3}$$

$$\begin{aligned}
\langle 0 | J_{\mu\nu}(0) | \psi_2 / \eta_{c2}(p) \rangle &= f_{\psi_2 / \eta_{c2}} \varepsilon_{\mu\nu}, \\
\langle 0 | J_{\mu\nu}(0) | \chi_{c1} / h_c(p) \rangle &= f_{\chi_{c1} / h_c} (p_\mu \varepsilon_\nu + p_\nu \varepsilon_\mu), \\
\langle 0 | J_{\mu\nu}(0) | \eta_c(p) \rangle &= f_{\eta_c} p_\mu p_\nu,
\end{aligned} \tag{4}$$

$$\begin{aligned}
\langle 0 | J_{\mu\nu\rho}(0) | \psi_3(p) \rangle &= f_{\psi_3} \varepsilon_{\mu\nu\rho}, \\
\langle 0 | J_{\mu\nu\rho}(0) | \chi_{c2}(p) \rangle &= f_{\chi_{c2}} (p_\mu \varepsilon_{\nu\rho} + p_\nu \varepsilon_{\rho\mu} + p_\rho \varepsilon_{\mu\nu}), \\
\langle 0 | J_{\mu\nu\rho}(0) | J/\psi / \psi_1(p) \rangle &= f_{J/\psi / \psi_1} (p_\mu p_\nu \varepsilon_\rho + p_\nu p_\rho \varepsilon_\mu + p_\rho p_\mu \varepsilon_\nu), \\
\langle 0 | J_{\mu\nu\rho}(0) | \chi_{c0}(p) \rangle &= f_{\chi_{c0}} p_\mu p_\nu p_\rho,
\end{aligned} \tag{5}$$

where the f_{ψ_1} , f_{ψ_2} , $f_{\eta_{c2}}$, f_{ψ_3} , $f_{\chi_{c0}}$, $f_{\chi_{c2}}$ and $f_{J/\psi}$ are decay constants, the ε_μ , $\varepsilon_{\mu\nu}$ and $\varepsilon_{\mu\nu\rho}$ are the polarization vectors of the charmonium states. Then we perform detailed tensor analysis and

isolate the ground state contributions,

$$\begin{aligned}
\Pi_{\mu\nu}(p) &= \Pi(p^2)\tilde{g}_{\mu\nu} + \Pi_0(p^2)p_\mu p_\nu, \\
&= \frac{f_{\psi_1}^2}{M_{\psi_1}^2 - p^2}\tilde{g}_{\mu\nu} + \dots, \\
\Pi_{\mu\nu\alpha\beta}(p) &= \Pi(p^2)P_{\mu\nu\alpha\beta} + \Pi_1(p^2)(\tilde{g}_{\mu\alpha}p_\nu p_\beta + \tilde{g}_{\mu\beta}p_\nu p_\alpha + \tilde{g}_{\nu\alpha}p_\mu p_\beta + \tilde{g}_{\nu\beta}p_\mu p_\alpha) + \Pi_0(p^2)p_\mu p_\nu p_\alpha p_\beta, \\
&= \frac{f_{\psi_2/\eta_{c2}}^2}{M_{\psi_2/\eta_{c2}}^2 - p^2}P_{\mu\nu\alpha\beta} + \dots, \\
\Pi_{\mu\nu\rho\alpha\beta\sigma}(p) &= \Pi(p^2)P_{\mu\nu\rho\alpha\beta\sigma} + \Pi_2(p^2)(P_{\nu\rho\beta\sigma}p_\mu p_\alpha + P_{\nu\rho\alpha\sigma}p_\mu p_\beta + P_{\nu\rho\alpha\beta}p_\mu p_\sigma + P_{\mu\rho\beta\sigma}p_\nu p_\alpha \\
&\quad + P_{\mu\rho\alpha\sigma}p_\nu p_\beta + P_{\mu\rho\alpha\beta}p_\nu p_\sigma + P_{\mu\nu\beta\sigma}p_\rho p_\alpha + P_{\mu\nu\alpha\sigma}p_\rho p_\beta + P_{\mu\nu\alpha\beta}p_\rho p_\sigma) \\
&\quad + \Pi_1(p^2)(\tilde{g}_{\mu\alpha}p_\nu p_\rho p_\beta p_\sigma + \tilde{g}_{\mu\beta}p_\nu p_\rho p_\alpha p_\sigma + \tilde{g}_{\mu\sigma}p_\nu p_\rho p_\alpha p_\beta + \tilde{g}_{\nu\alpha}p_\mu p_\rho p_\beta p_\sigma \\
&\quad + \tilde{g}_{\nu\beta}p_\mu p_\rho p_\alpha p_\sigma + \tilde{g}_{\nu\sigma}p_\mu p_\rho p_\alpha p_\beta + \tilde{g}_{\rho\alpha}p_\mu p_\nu p_\beta p_\sigma + \tilde{g}_{\rho\beta}p_\mu p_\nu p_\alpha p_\sigma + \tilde{g}_{\rho\sigma}p_\mu p_\nu p_\alpha p_\beta) \\
&\quad + \Pi_0(p^2)p_\mu p_\nu p_\rho p_\alpha p_\beta p_\sigma, \\
&= \frac{f_{\psi_3}^2}{M_{\psi_3}^2 - p^2}P_{\mu\nu\rho\alpha\beta\sigma} + \dots, \tag{6}
\end{aligned}$$

where

$$\begin{aligned}
\tilde{g}_{\mu\nu} &= -g_{\mu\nu} + \frac{p_\mu p_\nu}{p^2}, \\
P_{\mu\nu\alpha\beta} &= \frac{\tilde{g}_{\mu\alpha}\tilde{g}_{\nu\beta} + \tilde{g}_{\mu\beta}\tilde{g}_{\nu\alpha}}{2} - \frac{\tilde{g}_{\mu\nu}\tilde{g}_{\alpha\beta}}{3}, \\
P_{\mu\nu\rho\alpha\beta\sigma} &= \frac{1}{6}(\tilde{g}_{\mu\alpha}\tilde{g}_{\nu\beta}\tilde{g}_{\rho\sigma} + \tilde{g}_{\mu\alpha}\tilde{g}_{\nu\sigma}\tilde{g}_{\rho\beta} + \tilde{g}_{\mu\beta}\tilde{g}_{\nu\alpha}\tilde{g}_{\rho\sigma} + \tilde{g}_{\mu\beta}\tilde{g}_{\nu\sigma}\tilde{g}_{\rho\alpha} + \tilde{g}_{\mu\sigma}\tilde{g}_{\nu\alpha}\tilde{g}_{\rho\beta} + \tilde{g}_{\mu\sigma}\tilde{g}_{\nu\beta}\tilde{g}_{\rho\alpha}) \\
&\quad - \frac{1}{15}(\tilde{g}_{\mu\alpha}\tilde{g}_{\nu\rho}\tilde{g}_{\beta\sigma} + \tilde{g}_{\mu\beta}\tilde{g}_{\nu\rho}\tilde{g}_{\alpha\sigma} + \tilde{g}_{\mu\sigma}\tilde{g}_{\nu\rho}\tilde{g}_{\alpha\beta} + \tilde{g}_{\nu\alpha}\tilde{g}_{\mu\rho}\tilde{g}_{\beta\sigma} + \tilde{g}_{\nu\beta}\tilde{g}_{\mu\rho}\tilde{g}_{\alpha\sigma} + \tilde{g}_{\nu\sigma}\tilde{g}_{\mu\rho}\tilde{g}_{\alpha\beta} \\
&\quad + \tilde{g}_{\rho\alpha}\tilde{g}_{\mu\nu}\tilde{g}_{\beta\sigma} + \tilde{g}_{\rho\beta}\tilde{g}_{\mu\nu}\tilde{g}_{\alpha\sigma} + \tilde{g}_{\rho\sigma}\tilde{g}_{\mu\nu}\tilde{g}_{\alpha\beta}). \tag{7}
\end{aligned}$$

We choose the components $\Pi(p^2)$ to analyze the charmonium states with the quantum numbers $J^{PC} = 1^{--}, 2^{--}, 2^{-+}$ and 3^{--} without contaminations.

At the QCD side, we accomplish the operator product expansion up to the gluon condensate $\langle \frac{\alpha_s GG}{\pi} \rangle$ and three-gluon condensate $\langle g_s^3 GGG \rangle$, and the corresponding Feynman diagrams are displayed in Figs.1-2. In computation, we evaluate the integrals in momentum space, select the components $\Pi(p^2)$ associated with the particular structures in the correlation functions $\Pi_{\mu\nu}(p)$, $\Pi_{\mu\nu\alpha\beta}(p)$ and $\Pi_{\mu\nu\rho\alpha\beta\sigma}(p)$ to investigate the charmonium states with the spin-parity $J^P = 1^-, 2^-$ and 3^- respectively. At last, we determine the QCD spectral density $\rho(s)$ using dispersion relation.

We take quark-hadron duality below the continuum threshold s_0 and perform the Borel transformation with respect to the variable $P^2 = -p^2$ to acquire four QCD sum rules,

$$f^2 \exp\left(-\frac{M^2}{T^2}\right) = \int_{4m_c^2}^{s_0} ds \rho(s) \exp\left(-\frac{s}{T^2}\right), \tag{8}$$

where the T^2 are the Borel parameters, the decay constants $f = f_{\psi_1}, f_{\psi_2}, f_{\eta_{c2}}$ and f_{ψ_3} , the QCD spectral densities $\rho(s) = \rho_1(s), \rho_2^1(s), \rho_2^2(s)$ and $\rho_3(s)$,

$$\begin{aligned}
\rho_1(s) &= \frac{3(s - 4m_c^2)^2 \sqrt{s(s - 4m_c^2)}}{8\pi^2} + \left\langle \frac{\alpha_s GG}{\pi} \right\rangle \frac{24m_c^6 - 51sm_c^4 + 35s^2m_c^2 - 5s^3}{6s\sqrt{s(s - 4m_c^2)}} \\
&\quad + \langle g_s^3 GGG \rangle \frac{256m_c^6 - 1160sm_c^4 + 566s^2m_c^2 - 83s^3}{192\pi^2 s(s - 4m_c^2)\sqrt{s(s - 4m_c^2)}}, \tag{9}
\end{aligned}$$

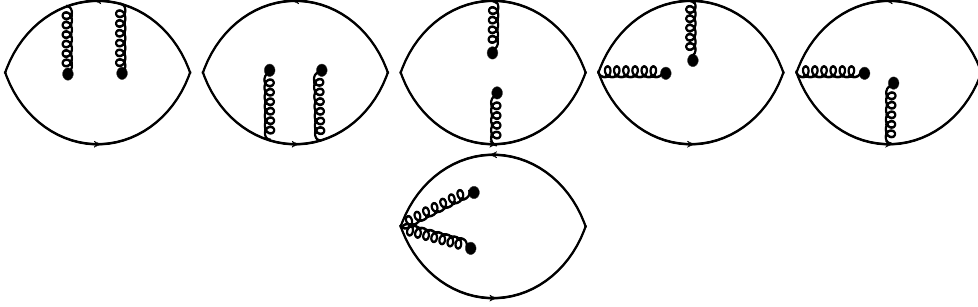


Figure 1: The Feynman diagrams contribute to the gluon condensate $\langle \frac{\alpha_s GG}{\pi} \rangle$.

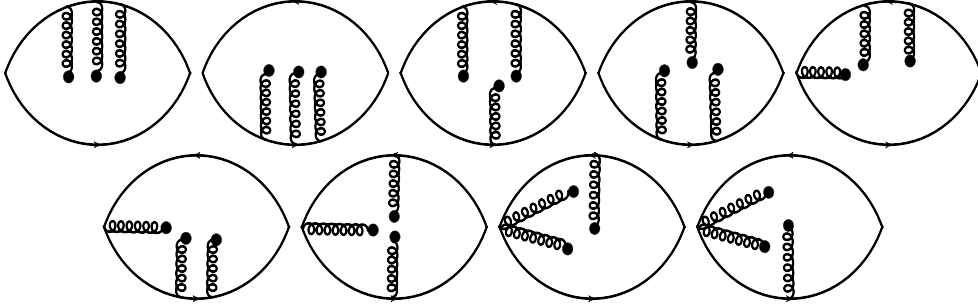


Figure 2: The Feynman diagrams contribute to the three-gluon condensate $\langle g_s^3 GGG \rangle$.

$$\begin{aligned} \rho_2^1(s) = & \frac{4(s-4m_c^2)^3(s+6m_c^2)}{5\pi^2\sqrt{s(s-4m_c^2)}} + \langle \frac{\alpha_s GG}{\pi} \rangle \frac{16(38m_c^6 - 61sm_c^4 - s^2m_c^2 + 3s^3)}{9s\sqrt{s(s-4m_c^2)}} \\ & + \langle g_s^3 GGG \rangle \frac{-192m_c^8 + 928sm_c^6 - 372s^2m_c^4 + 51s^3m_c^2 - 4s^4}{18\pi^2s^2(s-4m_c^2)\sqrt{s(s-4m_c^2)}}, \end{aligned} \quad (10)$$

$$\begin{aligned} \rho_2^2(s) = & \frac{(s-4m_c^2)^2\sqrt{s(s-4m_c^2)}}{5\pi^2} + \langle \frac{\alpha_s GG}{\pi} \rangle \frac{2(16m_c^6 - 30sm_c^4 - 3s^2m_c^2 + 2s^3)}{9s\sqrt{s(s-4m_c^2)}} \\ & + \langle g_s^3 GGG \rangle \frac{2m_c^4 + 3sm_c^2}{6\pi^2s\sqrt{s(s-4m_c^2)}}, \end{aligned} \quad (11)$$

$$\begin{aligned} \rho_3(s) = & \frac{9(s-4m_c^2)^3(s+3m_c^2)}{35\pi^2\sqrt{s(s-4m_c^2)}} + \langle \frac{\alpha_s GG}{\pi} \rangle \frac{120m_c^6 - 92sm_c^4 + 34s^2m_c^2 - 5s^3}{2s\sqrt{s(s-4m_c^2)}} \\ & + \langle g_s^3 GGG \rangle \frac{576m_c^8 - 992sm_c^6 + 284s^2m_c^4 + 6s^3m_c^2 - 7s^4}{16\pi^2s^2(s-4m_c^2)\sqrt{s(s-4m_c^2)}}, \end{aligned} \quad (12)$$

the $\rho_1(s)$, $\rho_2^1(s)$, $\rho_2^2(s)$ and $\rho_3(s)$ correspond the quark currents $J_\mu(x)$, $J_{\mu\nu}^1(x)$, $J_{\mu\nu}^2(x)$, and $J_{\mu\nu\rho}(x)$, respectively.

We extract the QCD sum rules for the masses of the D-wave charmonium states ψ_1 , ψ_2 , η_{c2} and ψ_3 by differentiating Eq.(8) with respect to $\frac{1}{T^2}$ and eliminating the decay constants,

$$M^2 = - \frac{\frac{d}{d\tau} \int_{4m_c^2}^{s_0} ds \rho(s) \exp(-\tau s)}{\int_{4m_c^2}^{s_0} ds \rho(s) \exp(-\tau s)} \Big|_{\tau=\frac{1}{T^2}}. \quad (13)$$

Input parameters	(I) [55, 56, 57]	(II) [59, 60]
$\langle \frac{\alpha_s GG}{\pi} \rangle$ (GeV ⁴)	0.012	0.022 ± 0.004
$\langle g_s^3 GGG \rangle$ (GeV ⁶)	0.045	0.616 ± 0.385

Table 2: The QCD input parameters, where the I and II denote the different values of the gluon condensate and three-gluon condensate.

3 Numerical results and discussions

We adopt the \overline{MS} (modified-minimal-subtraction) mass $m_c(m_c) = (1.275 \pm 0.025)$ GeV (from the Particle Data Group), which evolves with the energy scale μ according to the re-normalization group equation [58],

$$\begin{aligned}
m_c(\mu) &= m_c(m_c) \left[\frac{\alpha_s(\mu)}{\alpha_s(m_c)} \right]^{\frac{12}{33-2n_f}}, \\
\alpha_s(\mu) &= \frac{1}{b_0 t} \left[1 - \frac{b_1 \log t}{b_0^2 t} + \frac{b_1^2 (\log^2 t - \log t - 1) + b_0 b_2}{b_0^4 t^2} \right],
\end{aligned} \tag{14}$$

where $t = \log \frac{\mu^2}{\Lambda_{QCD}^2}$, $b_0 = \frac{33-2n_f}{12\pi}$, $b_1 = \frac{153-19n_f}{24\pi^2}$, $b_2 = \frac{2857 - \frac{5033}{9}n_f + \frac{325}{27}n_f^2}{128\pi^3}$, $\Lambda_{QCD} = 210$ MeV, 292 MeV and 332 MeV for the flavors $n_f = 5, 4$ and 3, respectively [58], and we take the flavor $n_f = 4$ and $m_c = \mu = (1.275 \pm 0.025)$ GeV. We adopt two sets of parameters for the gluon condensate $\langle \frac{\alpha_s GG}{\pi} \rangle$ and three-gluon condensate $\langle g_s^3 GGG \rangle$, as listed in Table 2.

The pole contributions are defined as,

$$\text{pole} = \frac{\int_{4m_c^2}^{s_0} ds \rho(s) \exp\left(-\frac{s}{T^2}\right)}{\int_{4m_c^2}^{\infty} ds \rho(s) \exp\left(-\frac{s}{T^2}\right)}. \tag{15}$$

In order to avoid parameter dependence to the utmost extent, we prefer the central value of the pole contributions 55% for all the charmonium states $\psi_1, \psi_2, \eta_{c2}$ and ψ_3 . To avoid contaminations from the higher resonances and continuum states, we adopt the constraint $\sqrt{s_0} = M + 0.45 \sim 0.65$ GeV for the continuum threshold parameters, and try to adjust the continuum threshold parameters to reproduce the charmonium masses M via trial and error, as the largest energy gap between the ground state and first radial excited state is 0.65 GeV for the charmonium states (i.e. $M_{\eta'_c} - M_{\eta_c} = 0.65$ GeV) [58]. The selection of the continuous threshold parameters both refer to the experimental results, and require ensuring that the operator product expansion at QCD side, the hadron sides and QCD sides are matched through dispersion relation to get the properties of the hadron states. The primary criteria are internal stability of the QCD sum rules, pole dominance, convergence of the OPE, and the existence of the Borel platform. These criteria take precedence over importing precise energy gaps predicted by other models, because the QCD sum rules extract hadron properties directly from correlation functions without assuming a specific dynamical model.

In the QCD spectral densities given in Eqs.(9)-(12), when the threshold $s = 4m_c^2$ is reached, the endpoint singularity arise from the factor the QCD spectral densities appear in the gluon condensate $\frac{1}{\sqrt{s(s-4m_c^2)}}$. Due to the minor contribution from the gluon condensate terms compared to the perturbative term as shown in Fig.3, we attempt to implement the routine replacements $s = 4m_c^2 \rightarrow s = 4m_c^2 + \Delta^2$ with $\Delta^2 = \frac{m_c^2}{2}, m_c^2, \frac{3m_c^2}{2}$ in numerical computations. The determination of numerical results for masses at three different Δ^2 values are consistent. To ensure as much consistency in parameters selection as possible, we adopted the $\Delta^2 = m_c^2$ substitution as used in our previous work [18, 19], then the corresponding Borel parameters and masses are obtained.

ψ	J^{PC}	$T^2(\text{GeV}^2)$	$\sqrt{s_0}(\text{GeV})$	pole	$M(\text{GeV})$	$f(\text{GeV}^4)$
$\psi_1(1^3D_1)$	1^{--}	2.9 – 3.5	4.30 ± 0.1	(43 – 68)%	$3.77^{+0.09}_{-0.09}$	$13.83^{+2.17}_{-1.99}$
$\psi_2(1^3D_2)$	2^{--}	3.2 – 3.8	4.40 ± 0.1	(48 – 70)%	$3.82^{+0.08}_{-0.09}$	$29.23^{+4.00}_{-3.69}$
$\eta_{c2}(1^1D_2)$	2^{-+}	3.0 – 3.6	4.40 ± 0.1	(47 – 71)%	$3.83^{+0.09}_{-0.08}$	$11.41^{+1.72}_{-1.57}$
$\psi_3(1^3D_3)$	3^{--}	3.2 – 3.8	4.40 ± 0.1	(45 – 68)%	$3.84^{+0.08}_{-0.08}$	$14.77^{+2.09}_{-1.92}$

Table 3: The spin-parity-charge-conjugation, Borel parameters, continuum threshold parameters, pole contributions, masses, decay constants of the charmonium states for the input parameters I.

ψ	J^{PC}	$T^2(\text{GeV}^2)$	$\sqrt{s_0}(\text{GeV})$	pole	$M(\text{GeV})$	$f(\text{GeV}^4)$
$\psi_1(1^3D_1)$	1^{--}	2.9 – 3.5	4.30 ± 0.1	(43 – 68)%	$3.77^{+0.09}_{-0.08}$	$13.82^{+2.18}_{-1.98}$
$\psi_2(1^3D_2)$	2^{--}	3.2 – 3.8	4.40 ± 0.1	(48 – 70)%	$3.82^{+0.08}_{-0.09}$	$29.29^{+4.00}_{-3.69}$
$\eta_{c2}(1^1D_2)$	2^{-+}	3.0 – 3.6	4.40 ± 0.1	(47 – 71)%	$3.83^{+0.09}_{-0.09}$	$11.64^{+1.72}_{-1.58}$
$\psi_3(1^3D_3)$	3^{--}	3.2 – 3.8	4.40 ± 0.1	(45 – 68)%	$3.84^{+0.09}_{-0.07}$	$14.94^{+2.11}_{-1.94}$

Table 4: The spin-parity-charge-conjugation, Borel parameters, continuum threshold parameters, pole contributions, masses, decay constants of the charmonium states for the input parameters II.

We define the normalized contributions $D(n)$,

$$D(n) = \frac{\int_{4m_c^2}^{s_0} ds \rho_{QCD,n}(s) \exp\left(-\frac{s}{T^2}\right)}{\int_{4m_c^2}^{s_0} ds \rho_{QCD}(s) \exp\left(-\frac{s}{T^2}\right)}, \quad (16)$$

where the $\rho_{QCD,n}(s)$ are the QCD spectral densities $\rho_1(s)$, $\rho_2^1(s)$, $\rho_2^2(s)$ and $\rho_3(s)$ involving the vacuum condensates of dimension n . In Fig.3, we plot the contributions of the vacuum condensates $D(n)$ for the charmonium states ψ_1 , ψ_2 , η_{c2} and ψ_3 for the central values of the input parameters given in Table 2, which reveals that the perturbative terms account for the major contributions, the three-gluon condensate $\langle g_s^3 GGG \rangle$ contributions are minimal, and they have the hierarchy $|D(0)| \gg |D(4)| \geq |D(6)|$, the operator product expansion converges rather well.

We plot the charmonium masses with variations of the Borel parameters T^2 in Fig.4, the selected ranges of the Borel platforms are shown by the two vertical lines, while the experimental masses are represented by the horizontal dashed lines. We obtain the central value of the masses based on the pole contribution 50%, then consider the uncertainties of the input parameters, and take the pole contribution $\leq 70\%$ ($\geq 40\%$) to determine the lower (upper) boundary of the Borel windows. It can be seen from Figs.3-4 that the contributions of the vacuum condensates and the masses remain stable in the Borel windows.

Although the QCD input parameters I and II differ greatly in the value of the three-gluon condensate $\langle g_s^3 GGG \rangle$, the predicted masses are identical. Moreover, the Borel parameter, the continuum threshold parameter and pole are also exactly the same with the only minor deviations occurring in the decay constants. After taking account of the uncertainties, we display the masses and decay constants in Tables 3-4. The uncertainties in our predictions for the masses are derived by all input parameters through the analytical expressions $\delta = \sqrt{\sum_i \left(\frac{\partial M}{\partial x_i}\right)^2 (x_i - x)^2}$. The uncertainties are propagated using standard error analysis, where M represent the masses, x_i denote the input parameters charm-quark mass, gluon condensates, three-gluon condensates, continuum threshold, and x denote the the central values of these parameters. Since it is difficult to find the analytic expressions of the partial derivatives $\frac{\partial M}{\partial x_i}$, we carry out the approximate numerical calculations and estimate the corresponding uncertainties $\delta \approx \sqrt{\sum_i |M(x \pm \Delta x_i) - M(x)|^2}$ via numerical

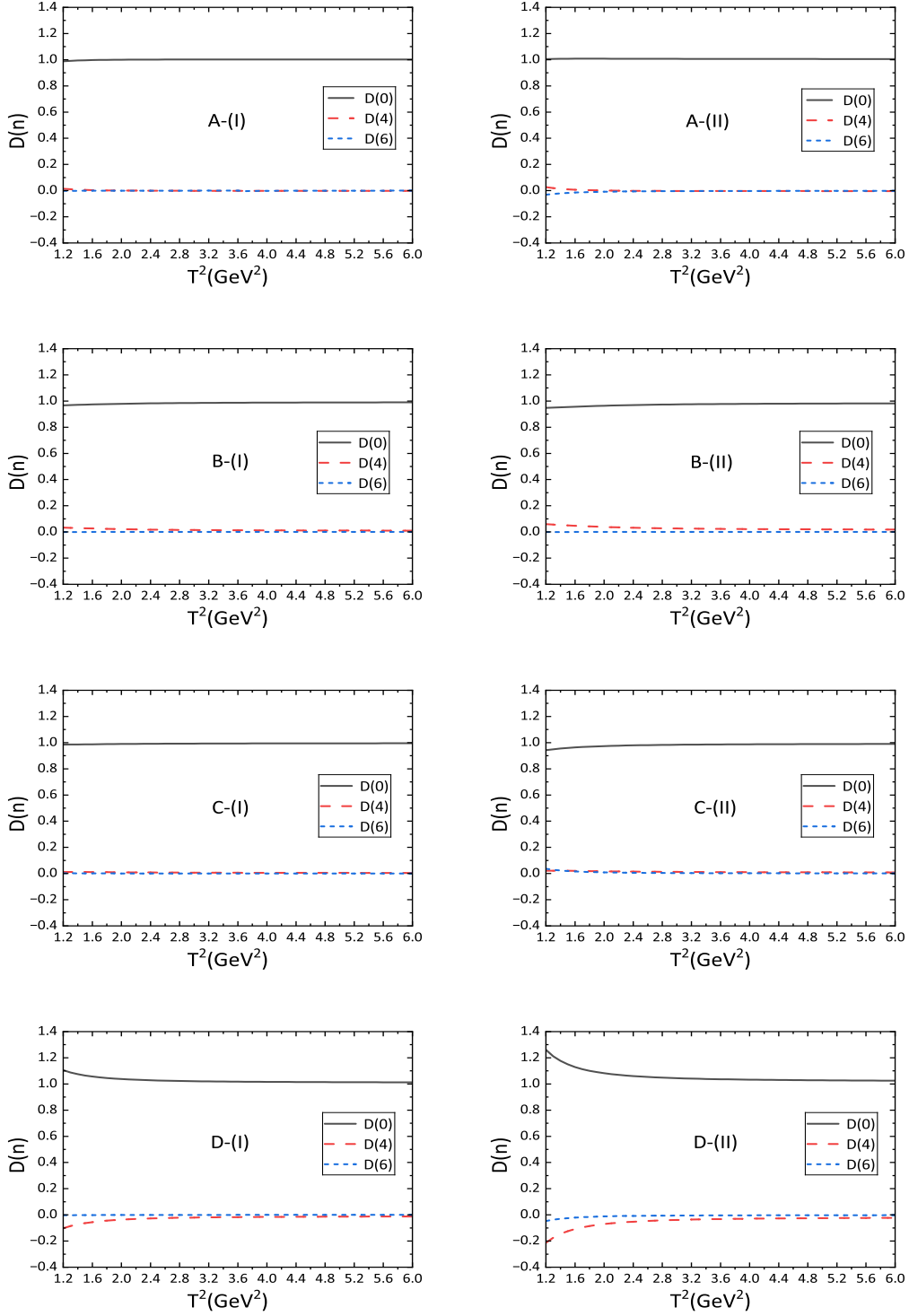


Figure 3: The contributions of the vacuum condensates of dimension n with variations of the Borel parameters T^2 of the input parameters are set to central values, where the A , B , C and D denote ψ_1 , ψ_2 , η_{c2} and ψ_3 charmonium states, respectively.

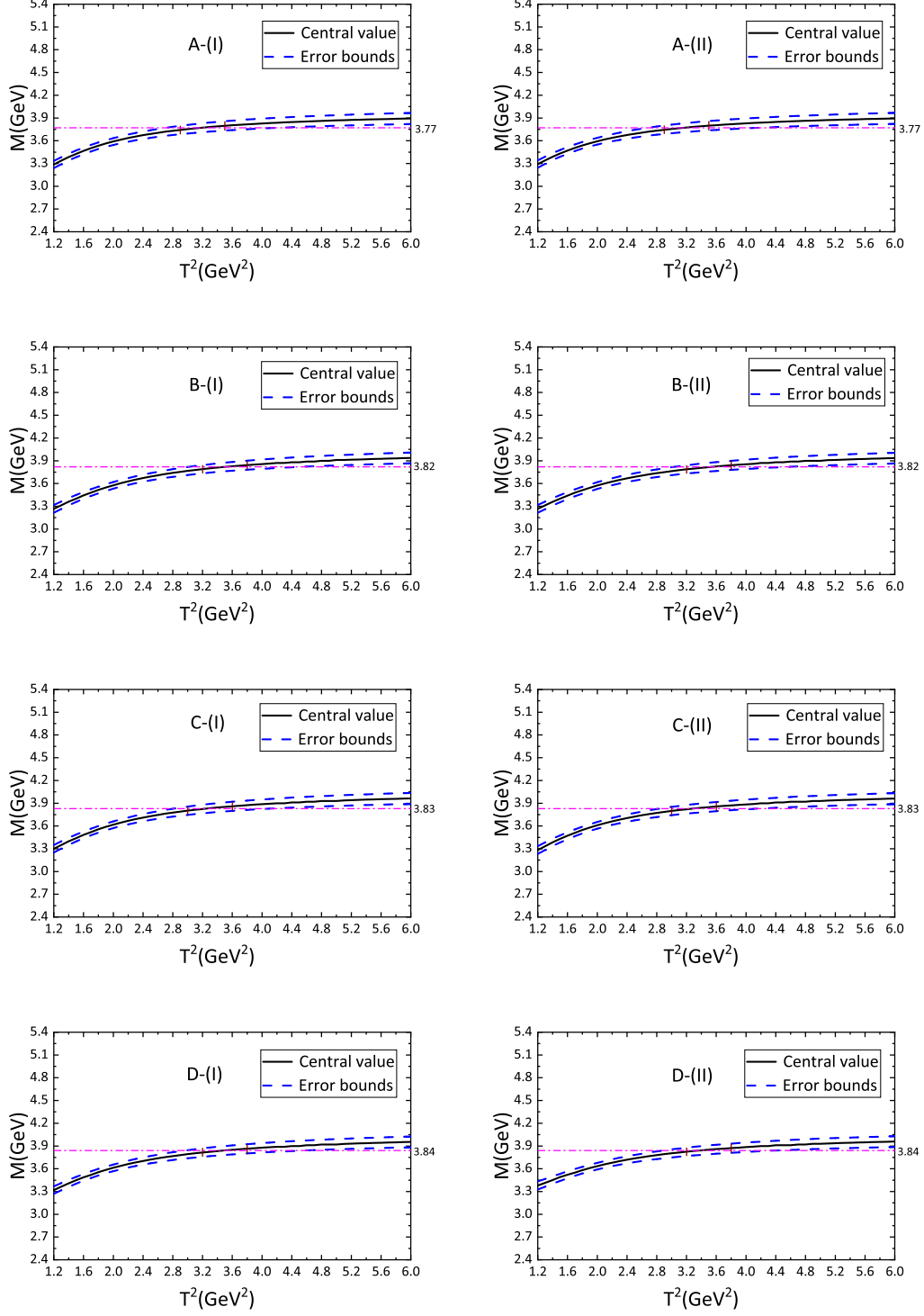


Figure 4: The masses of the charmonium states with variations of the Borel parameters T^2 , where the A, B, C and D denote ψ_1 , ψ_2 , η_{c2} and ψ_3 charmonium states, respectively.

uncertainty	Δx_i	$\Delta M_{\psi_1(1^3D_1)}$	$\Delta M_{\psi_2(1^3D_2)}$	$\Delta M_{\eta_{c2}(1^1D_2)}$	$\Delta M_{\psi_3(1^3D_3)}$
m_c	$\pm 0.025 \text{ GeV}$	$\pm 22.07 \text{ MeV}$	$\pm 23.31 \text{ MeV}$	$\pm 22.58 \text{ MeV}$	$\pm 22.24 \text{ MeV}$
$\sqrt{s_0}$	$\pm 0.1 \text{ GeV}$	$\pm 54.54 \text{ MeV}$	$\pm 52.55 \text{ MeV}$	$\pm 53.04 \text{ MeV}$	$\pm 53.75 \text{ MeV}$
T^2	$\pm 0.3 \text{ GeV}$	$\pm 26.95 \text{ MeV}$	$\pm 29.11 \text{ MeV}$	$\pm 28.85 \text{ MeV}$	$\pm 24.99 \text{ MeV}$

Table 5: The mass uncertainties of the parameters variation for input parameter I.

uncertainty	Δx_i	$\Delta M_{\psi_1(1^3D_1)}$	$\Delta M_{\psi_2(1^3D_2)}$	$\Delta M_{\eta_{c2}(1^1D_2)}$	$\Delta M_{\psi_3(1^3D_3)}$
m_c	$\pm 0.025 \text{ GeV}$	$\pm 21.92 \text{ MeV}$	$\pm 23.51 \text{ MeV}$	$\pm 22.69 \text{ MeV}$	$\pm 22.15 \text{ MeV}$
$\sqrt{s_0}$	$\pm 0.1 \text{ GeV}$	$\pm 54.36 \text{ MeV}$	$\pm 52.45 \text{ MeV}$	$\pm 53.06 \text{ MeV}$	$\pm 53.62 \text{ MeV}$
T^2	$\pm 0.3 \text{ GeV}$	$\pm 26.78 \text{ MeV}$	$\pm 26.67 \text{ MeV}$	$\pm 29.30 \text{ MeV}$	$\pm 23.95 \text{ MeV}$
$\langle \frac{\alpha_s GG}{\pi} \rangle$	$\pm 0.004 \text{ GeV}^4$	$\pm 0.22 \text{ MeV}$	$\pm 1.31 \text{ MeV}$	$\pm 0.61 \text{ MeV}$	$\pm 2.61 \text{ MeV}$
$\langle g_s^3 GGG \rangle$	$\pm 0.385 \text{ GeV}^6$	$\pm 1.45 \text{ MeV}$	$\pm 0.33 \text{ MeV}$	$\pm 1.49 \text{ MeV}$	$\pm 1.68 \text{ MeV}$

Table 6: The mass uncertainties of the parameters variation for input parameter II.

differentiation. To elucidate the origins of the mass uncertainties quoted in Tables 3-4, we examine the individual impacts of the charm-quark mass variation m_c , the gluon condensates $\langle \frac{\alpha_s GG}{\pi} \rangle$ and three gluon condensates $\langle g_s^3 GGG \rangle$, and the Borel windows T^2 . Tables 5-6 display the resulting masses shift when each parameter is varied independently while others are fixed at their central values. The gluon condensates contribute negligibly (a few MeV), consistent with the convergent OPE and the perturbative dominance shown in Fig.3 which confirming the reliability of our uncertainties. It is noteworthy that our predicted mass results will be based on the central values as far as possible and subsequently compared against future experimental or other theoretical results.

Our prediction $M_{\psi_1} = 3.77 \pm 0.09 \text{ GeV}$ favors assigning the conventional $\psi(3770)$ (rather than the $\mathcal{R}(3780)$ reported by the BESIII collaboration [16, 17]) as the D-wave charmonium ψ_1 . Our result of $M_{\psi_1(1^3D_1)}$ supports the dominance of the D-wave Fock component for $\psi(3770)$. The mass of $\psi(3770)$ lies significantly above $\psi(2S)$. Although the consideration of S-D mixing effects on vector charmonia can interpret their experimental di-electric widths [61], the S-wave admixture were very large, such agreement would be unlikely. The predicted mass $M_{\psi_2} = 3.82 \pm 0.09 \text{ GeV}$ is consistent with the observation of the Belle, BESIII and LHCb collaborations [20, 21, 22, 23, 24], and favors the identification ψ_2 indeed. While the 1^1D_2 charmonium state has not been discovered yet, we estimate the mass to be $M_{\eta_{c2}} = 3.83 \pm 0.09 \text{ GeV}$, which is expected to be observed at the BESIII, LHCb, Belle II collaborations in the future. Furthermore, we obtain the mass $M_{\psi_3} = 3.84 \pm 0.08 \text{ GeV}$, and tentatively identify the $X(3842)(\psi_3(3842))$ as the 1^3D_3 charmonium state [25]. We can take the decay constants $f_{\psi_1/\psi_2/\eta_{c2}/\psi_3}$ are elementary input parameters to study the strong decays and radiative decays to make the identifications in a more robust way.

The comparison of our mass predictions with those from other theoretical approaches, as summarized in Table 7. The potential models generally predict masses in the range of $3.77 - 3.84 \text{ GeV}$, if we consider the uncertainty ranges, the predictions from these methods fall within our calculated error bands. Therefore, the following discussion will focus on comparison of the central values, for the ψ_1 state, the quark model predictions are generally higher than our results, which may be attributed to inherent model dependencies. Our central values of the unobserved η_{c2} is closed to some quark models. This concordance between the methods is particularly noteworthy and reinforces the credibility of approaches. Further experimental data are essential to advance our understanding of the D-wave charmonium systems. In particular, the observation of the η_{c2} state and more precise measurements of masses, widths, and decay channels for the charmonia are crucial to test theoretical predictions.

The decay constant is a crucial parameter in the calculation of strong, leptonic, semileptonic,

	ref.	$M_{\psi_1(1^3D_1)}$ (GeV)	$M_{\psi_2(1^3D_2)}$ (GeV)	$M_{\eta_{c2}(1^1D_2)}$ (GeV)	$M_{\psi_3(1^3D_3)}$ (GeV)
QCD sum rules	this work	3.77	3.82	3.83	3.84
Bethe-Salpeter equations	[32]	-	3.739	3.806	3.896
nonrelativistic potential model	[39]	3.785	3.800	3.799	3.806
	[40]	3.787	3.798	3.796	3.799
(linear potential model)	[41]	3.787	3.807	3.806	3.811
(screened potential model)	[41]	3.792	3.807	3.805	3.808
unquenched potential model	[45]	3.830	3.848	3.848	3.859
GI model	[39]	3.819	3.838	3.837	3.849
Coulomb plus linear potential model	[43]	3.815	3.814	3.806	3.798
Cornell potential model	[46]	3.775	3.772	3.765	3.755
Cornell coupled-channel model	[14]	-	3.831	3.838	3.868
Cornell potential coupled relativistic correction	[47]	3.785	3.800	3.780	3.806
QCD-motivated relativistic quark model	[49]	3.783	3.795	3.807	3.813
other potential model	[50]	3.781	3.800	3.799	3.805
	[53]	3.804	3.824	3.824	3.831

Table 7: The mass of the D-wave charmonia.

and radiative decays. For instance, in Ref.[62], the decay constants f_{ψ_1} , f_{ψ_2} , $f_{\eta_{c2}}$, f_{ψ_3} presented in this work is employed within the framework of three-point correlation functions to compute the semileptonic decay width of D-wave charmonia. There is a scarcity of research dedicated to direct compute the decay constants for D-wave charmonia [63]. Our calculated constants are not merely numerical outputs but are key phenomenological parameters that bridge the gap between mass predictions and the future analysis of decay widths and branching ratios.

The values of the non-perturbative vacuum condensates, particularly the triple-gluon condensate $\langle g_s^3 GGG \rangle$, are not as precisely determined as the fundamental parameters like the charm quark mass m_c . Different extraction methods from QCD sum rules analyse or phenomenological fits can lead to differing numerical estimates. The predicted masses for all four D-wave charmonium states remain remarkably stable and consistent between the two parameter sets, as detailed in Tables 3 and 4, the variations are well within the quoted uncertainties. This demonstrates that our mass predictions are dominated by the perturbative contribution and are not sensitive to the specific choice of the gluon condensate values and the triple-gluon condensate. While the masses are robust, we observe the minor sensitivity in the decay constants, the parameter sets I and II are considered.

4 Conclusion

In this work, we perform a systematic analysis of the conventional D-wave charmonium states ψ_1 , ψ_2 , η_{c2} and ψ_3 in the framework of the QCD sum rules. We carry out the operator product up to the condensates of dimension-6, which includes both the gluon condensate $\langle \frac{\alpha_s GG}{\pi} \rangle$ and the three-gluon condensate $\langle g_s^3 GGG \rangle$. Notably, despite significant differences between the values of the three-gluon condensate in the two adopted parameter sets I and II adopted, the resulting mass predictions remain remarkably stable and consistent. This robustness underscores the reliability of the QCD sum rules and the dominant role of the perturbative contributions. We observe that the predicted

masses favor identifying the $\psi(3770)$, $\psi_2(3823)$ and $\psi_3(3842)$ as the D-wave charmonium states 1^3D_1 , 1^3D_2 and 1^3D_3 , respectively. Since the $\eta_{c2}(1^1D_2)$ has not been observed experimentally yet, we make prediction to be confronted to experimental data in the future. Meanwhile, the obtained decay constants can serve as elementary input parameters in subsequent study of the strong decays, leptonic and radiative decays to make the identifications in a more robust way.

Acknowledgements

This work is supported by National Natural Science Foundation, Grant Number 12175068 and the Fundamental Research Funds for the Central Universities (2025MS177).

References

- [1] J. J. Aubert *et al.*, Phys. Rev. Lett. **33** (1974) 1404.
- [2] J. E. Augustin *et al.*, Phys. Rev. Lett. **33** (1974) 1406.
- [3] S. K. Choi *et al.*, Phys. Rev. Lett. **91** (2003) 262001.
- [4] R. Partridge *et al.*, Phys. Rev. Lett. **45** (1980) 1150.
- [5] C. Edwards *et al.*, Phys. Rev. Lett. **48** (1982) 70.
- [6] C. J. Biddick *et al.*, Phys. Rev. Lett. **38** (1977) 1324.
- [7] W. M. Tanenbaum *et al.*, Phys. Rev. Lett. **35** (1975) 1323.
- [8] J. S. Whitaker *et al.*, Phys. Rev. Lett. **37** (1976) 1596.
- [9] R. Brandelik *et al.*, Phys. Lett. **B76** (1978) 361.
- [10] J. Siegrist *et al.*, Phys. Rev. Lett. **36** (1976) 700.
- [11] V. A. Novikov, L. B. Okun, M. A. Shifman, A. I. Vainshtein, M. B. Voloshin and V. I. Zakharov, Phys. Rept. **41** (1978) 1.
- [12] S. Godfrey and N. Isgur, Phys. Rev. **D32** (1985) 189.
- [13] D. Ebert, R. N. Faustov and V. O. Galkin, Phys. Rev. **D67** (2003) 014027.
- [14] E. J. Eichten, K. Lane and C. Quigg, Phys. Rev. **D69** (2004) 094019.
- [15] P. A. Rapidis *et al.*, Phys. Rev. Lett. **39** (1977) 526.
- [16] K. Abe *et al.*, Phys. Rev. Lett. **93** (2004) 051803.
- [17] M. Ablikim *et al.*, Phys. Rev. Lett. **133** (2024) 241902.
- [18] Z. G. Wang, Int. J. Mod. Phys. **A37** (2022) 2250166.
- [19] Z. G. Wang, Nucl.Phys. **B973** (2021) 115579.
- [20] V. Bhardwaj *et al.*, Phys. Rev. Lett. **111** (2013) 032001.
- [21] M. Ablikim *et al.*, Phys. Rev. Lett. **115** (2015) 011803.
- [22] R. Aaij *et al.*, JHEP **08** (2020) 123.
- [23] M. Ablikim *et al.*, Phys. Rev. Lett. **129** (2022) 102003.

- [24] M. Ablikim *et al.*, JHEP **02** (2023) 171.
- [25] R. Aaij *et al.*, JHEP **07** (2019) 035.
- [26] M. Ablikim *et al.*, Phys.Rev.Lett. **132** (2024) 191902.
- [27] M. Ablikim *et al.*, Phys. Rev. Lett. **127** (2021) 082002.
- [28] Z. G. Wang, Eur. Phys. J. **C75** (2015) 25.
- [29] Z. G. Wang, Eur. Phys. J. **C75** (2015) 427.
- [30] Z. G. Wang, Nucl. Phys. **A957** (2017) 85.
- [31] G. L. Yu and Z. G. Wang, Int. J. Mod. Phys. **A34** (2019) 1950151.
- [32] C. S. Fischer, S. Kubrak and R. Williams, Eur. Phys. **JA51** (2015) 10.
- [33] Z. G. Wang, Nucl. Phys. **B1007** (2024) 116661.
- [34] Z. G. Wang, Int. J. Mod. Phys. **A36** (2021) 2150107.
- [35] Z. G. Wang, Phys. Rev. **D102** (2020) 014018.
- [36] Z. G. Wang, Front. Phys. **21** (2026) 016300.
- [37] Z. G. Wang, Phys. Rev. **D101** (2020) 074011.
- [38] T. Barnes and S. Godfrey, Phys. Rev. **D69** (2004) 054008.
- [39] T. Barnes, S. Godfrey and E. S. Swanson, Phys. Rev. **D72** (2005) 054026.
- [40] B. Q. Li and K. T. Chao, Phys. Rev. **D79** (2009) 094004.
- [41] W. J. Deng, H. Liu, L. C. Gui and X. H. Zhong, Phys. Rev. **D95** (2017) 034026.
- [42] A. E. Bernardini and C. Dobrigkeit, J. Phys. G **29** (2003)1439.
- [43] R. Chaturvedi and A. Kumar Rai, Eur. Phys. J. Plus **133** (2018) 220.
- [44] C. A. Bokade and Bhaghyesh, Phys. Rev. **D111** (2025) 014030.
- [45] J. Z. Wang, D. Y. Chen, X. Liu and T. Matsuki, Phys. Rev. **D99** (2019) 114003.
- [46] N. R. Soni, B. R. Joshi, R. P. Shah, H. R. Chauhan and J. N. Pandya, Eur. Phys. J. **C78** (2018) 592.
- [47] R. Chaturvedi and A. K. Rai, Int. J. Theor. Phys. **59** (2020) 3508.
- [48] Z. L. Man, C. R. Shu, Y. R. Liu and H. Chen, Eur. Phys. J. **C84** (2024) 810.
- [49] D. Ebert, R. N. Faustov and V. O. Galkin, Eur. Phys. J. **C71** (2011) 1825.
- [50] M. A. Sultan, N. Akbar, B. Masud and F. Akram, Phys. Rev. **D90** (2014) 054001.
- [51] V. Kher and A. K. Rai, Chin. Phys. **C42** (2018) 083101.
- [52] T. Bhavsar, M. Shah and P. C. Vinodkumar, Eur. Phys. J. **C78** (2018) 227.
- [53] S. F. Radford and W. W. Repko, Phys. Rev. **D75** (2007) 074031.
- [54] J. J. Zhu and M. L. Yan, hep-ph/9903349.

- [55] M. A. Shifman, A. I. Vainshtein and V. I. Zakharov, Nucl. Phys. **B147** (1979) 385; Nucl. Phys. **B147** (1979) 448.
- [56] L. J. Reinders, H. Rubinstein and S. Yazaki, Phys. Rept. **127** (1985) 1.
- [57] P. Colangelo and A. Khodjamirian, hep-ph/0010175.
- [58] S. Navas *et al.*, Phys. Rev. **D110** (2024) 030001.
- [59] S. Narison, Phys. Lett. B **706** (2012) 412.
- [60] S. Narison, Phys. Lett. B **707** (2012) 259.
- [61] Z. L. Man, C. R. Shu, Y. R. Liu and H. Chen, Eur. Phys. J. C **84** (2024) 810.
- [62] J. Lu, D. Y. Chen, G. L. Yu and Z. G. Wang, Phys. Lett. **B872** (2026) 140057.
- [63] A. Krassnigg and T. Hilger, J. Phys. Conf. Ser. **1024** (2018) 012010.